scientific reports

Check for updates

OPEN

6-hydroxygenistein attenuates hypoxia-induced injury via activating Nrf2/HO-1 signaling pathway in PC12 cells

Pengpeng Zhang[1,2], Jie Zhang[2], Chuan Ma[2], Huiping Ma[2]✉ & Linlin Jing[1,2]✉

4′,5,6,7-tetrahydoxyisoflavone (6-hydroxygenistein, 6-OHG) is a hydroxylated derivative of genistein with excellent antioxidant activity, but whether 6-OHG can protect hypoxia-induced damage is unclear. The objective of current study was to evaluate the protective effect and underling mechanism of 6-OHG against hypoxia-induced injury via network pharmacology and cellular experiments. 6-OHG-related and hypoxia injury-related targets were screened by public databases. The intersected targets were used for constructing PPI network and performing GO and KEGG functional analysis. We induced injury in PC12 cells under hypoxia conditions and observed the effects and molecular mechanisms of 6-OHG on cellular damage. Network pharmacological analysis predicted that 6-OHG delayed hypoxia injury by mitigating oxidative stress, inflammatory response and apoptosis. Cellular experiments suggested that 6-OHG treatment mitigated cell damage, enhanced cell viability, reduced ROS production and MDA level, increased SOD and CAT activities and elevated GSH level in PC12 cell exposed to hypoxia. Additionally, 6-OHG treatment reduced the TNF-α and IL-6 levels and elevated the IL-10 content, while downregulated the NF-κB and TNF-α expressions. 6-OHG also inhibited the caspase-3 and −9 activation and the Bax and cleaved caspase-3 expressions, and elevated the Bcl-2 expression. Moreover, 6-OHG remarkably enhanced Nrf2 nuclear translocation and increased HO-1 expression. Molecular docking also proved the strong binding affinities of 6-OHG with Nrf2 and HO-1. Furthermore, ML385, a specific Nrf2 inhibitor, eliminated the beneficial effects of 6-OHG. In summary, 6-OHG can alleviate hypoxia-induced injury in PC12 cells through activating Nrf2/HO-1 signaling pathway and may be developed as candidate for preventing neuro-damage induced by hypoxia.

Keywords 6-hydroxygenistein, Hypoxia injury, Oxidative stress, Nrf2/HO-1 signaling pathway, Inflammatory response, Apoptosis

Abbreviations

6-OHG	6-hydroxygenistein
PC12	Rat pheochromocytoma
GO	Gene Ontology
KEGG	Kyoto Encyclopedia of Genes and Genomes
ROS	Reactive oxygen species
MDA	Malondialdehyde
SOD	Superoxide dismutase
CAT	Catalase
GSH	Glutathione
IL-6	Interleukin-6
IL-10	Interleukin-10
TNF-α	Tumor necrosis factor-α
Nrf2	Nuclearfactor erythroidderived 2-like 2
HO-1	Heme oxygenase 1

[1]Department of Pharmacy, the First Affiliated Hospital of Xi'an Jiaotong University, NO.277 Yanta West Road, Yanta District, Xi'an 710061, Shaanxi, People's Republic of China. [2]Department of Pharmacy, the 940th Hospital of Joint Logistics Support force of PLA, NO.333 Binhe South Road, Qilihe District, Lanzhou 730050, Gansu, People's Republic of China. ✉email: lzu_mahp@lzu.edu.cn; jinglinlin@xjtufh.edu.cn

ATP	Adenosine triphosphate
LDH	Lactate dehydrogenase
NF-κB	Nuclear factor kappa-light-chain-enhancer of activated B cells
GSH-Px	Glutathione peroxidase
CNS	Central nervous system
HPLC	High-performance liquid chromatographic
DCFH-DA	2,7-Dichlorofluorescein diacetate
DAPI	4',6-diamidino-2-phenylindole
DMEM	Dulbecco's Modified Eagle Medium
FBS	Fetal bovine serum
PBS	Phosphate buffered saline
OD	Optical density
TUNEL	Terminal deoxynucleotidyl transferase-mediated deoxy-UTP (dUTP) nick end labeling
SDS-PAGE	Sodium dodecyl sulfate–polyacrylamide gel electrophoresis
PVDF	Polyvinylidene difluoride
ECL	Enhanced chemiluminescence
BP	Biological process
CC	Cellular composition
MF	Molecular function
PPI	Protein-protein interaction
PHD	Prolyl Hydroxylase
Mcl-1	Myeloid cell leukemia-1
Bcl-2	b-cell lymphoma-2
Bax	Bcl-2-associated X protein
Bak	Bcl-2 antagonist/killer protein
NQO1	NAD(P)H quinone oxidoreductase
AREs	Antioxidant response elements

Molecular oxygen (O_2) is essential for most species on earth. Cells consume oxygen to synthesize ATP, which is used to maintain normal cellular physiological functions. Hypoxia, defined as insufficient oxygen supply, is a major stressor, especially for central nervous system (CNS) due to its high metabolic utilization of oxygen. Hypoxia has been associated with cognitive dysfunction[1], depression[2], and a decline in health-related quality of life[3]. Therefore, effective strategies to minimize hypoxia-induced neurological damage are essential.

Although the molecular mechanisms of hypoxic injury are not fully understood, there is growing evidence that oxidative stress, neuroinflammation, and apoptosis play key roles in hypoxia-induced neuronal injury. Compounds with the abilities of reducing oxidative stress, inflammation and apoptosis have been reported to be effective in treating hypoxia induced injury[4–6].

4',5,6,7-tetrahydoxyisoflavone (6-hydroxygenistein, 6-OHG, Fig. 1A) is a hydroxylated derivative of genistein found in fermented soybean or microbial fermentation broth[7], which has emerged as an important part of people's dietary food because of the unique flavors and improved health benefit[8]. Its molecule contains four phenolic hydroxyl groups and *ortho*-dihydroxy structure in the A ring, all of which contribute to its excellent free radicals scavenging activities in vitro[9]. In addition, 6-OHG also exhibits anticancer[10], antimelanogenesis[11], and hepatoprotective[12] activities. However, whether 6-OHG protects against hypoxia induced injury and the underlying mechanisms have yet to be revealed.

Network pharmacology is an emerging interdisciplinary discipline based on the theory of systems biology, using bioinformatics and network analysis methods to analyze biological systems and study the potential mechanisms of multi-target drugs at the system level[13]. Rat pheochromocytoma (PC12) cells, which have the property of neurite growth, have been widely used in neuroscience research[14]. In the current study, network pharmacology and in vitro experiments on PC12 cell were employed to clarify the protective effects and the underling mechanism of 6-OHG against hypoxia-induced injury. This study provides a scientific basis for understanding the protective effects of 6-OHG against hypoxic neuronal injury at the molecular level.

Materials and methods

Network pharmacology research

Construction of networks

The SwissTargetPrediction (http://www.swisstargetprediction.ch/), Similarity ensemble approach (https://sea.bkslab.org/), PharmMapper (http://www.lilab-ecust.cn/pharmmapper/), and SuperPred (https://prediction.charite.de/) databases were used to retrieve the potential targets of 6-OHG. A search for "hypoxia injury" and "hypoxia damage" was performed in the GeneCards (https://www.genecards.org/) and OMIM (https://www.omim.org/) databases to identify candidate targets. The intersection targets were obtained and visualized by Venny 2.1. Then those overlapped targets were used for PPI analysis by importing into the STRING (https://string-db.org) database. Cytoscape 3.9.0 was used to visualize the results.

Gene Ontology (GO) and Kyoto Encyclopedia of genes and genomes (KEGG) pathway enrichment analysis[15]

To elucidate the potential targets of 6-OHG against hypoxia injury, DAVID database (https://david.ncifcrf.gov/) was utilized for GO and KEGG enrichment analyses of the overlapped targets. Then, visualization was carried out using the R 4.4.1.

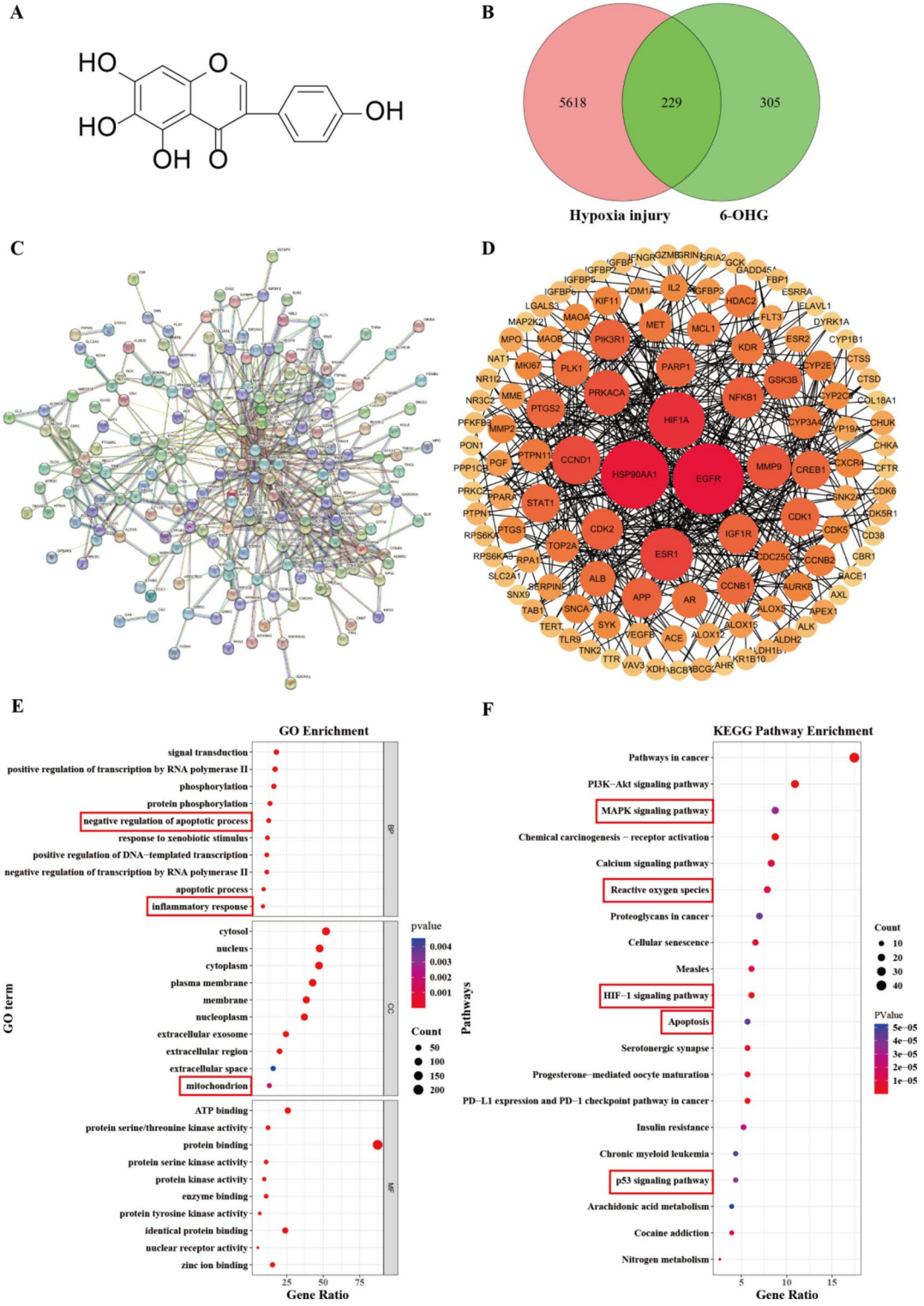

Fig. 1. Network pharmacological analysis of 6-OHG in treating hypoxia-induced injury. (**A**) Structure of 6-hydroxygenistein (6-OHG). (**B**) Venn diagram of targets shared by both 6-OHG and hypoxia injury. (**C**) PPI network by STRING. (**D**) PPI network by Cytoscape. (**E**) GO functional enrichment analysis (**F**) KEGG pathway enrichment analysis.

Chemicals and regents

6-OHG (high-performance liquid chromatographic (HPLC purity > 98%)) was synthesized in accordance with our earlier published method[9]. Rutin (HPLC purity > 98%, 20121106), purchased from Shaanxi Ci Yuan Biotechanology Co., Ltd (Xi'an, China) and was used as positive control[16]. ML385 (HY-100523), a selective Nrf2

inhibitor, was obtained from Medchem Express (Shanghai, China). 6-OHG, rutin and ML385 were prepared as a 10 mM stock solution with dimethyl sulfoxide (DMSO) and then diluted with culture medium to the desired concentration. The content of DMSO in final culture medium didn't surpass 0.1%. 2,7-Dichlorofluorescein diacetate (DCFH-DA, E004-1-1) was provided by Nanjing Jiancheng Bioengineering Research Institute (Nanjing, China) for measurement of ROS. 4',6-diamidino-2-phenylindole (DAPI, C1005) was purchased from Byotime Biotechnology Company (Hangzhou, China) for labeling the nuclei. Dulbecco's Modified Eagle Medium (DMEM, C7078), Fetal bovine serum (FBS, C7074), phosphate buffered saline (PBS, C01-01002), 0.25% Trypsin-Ethylenediamine tetraacetic acid (C7042), 1% penicillin/streptomycin (C7072) and Cell counting kit-8 (CCK-8, BA00208) were provided by Bioss Biotechnology (Hangzhou, China). The primary antibodies against VEGF (ab46154), NF-κB (ab220803), TNF-α (ab183218), Bax (ab182733), Bcl-2 (ab196495), cleaved caspase-3 (ab214430) and β-actin (ab8227) were provided by Abcam (Cambridge, UK). The primary antibodies against HIF-1α (D2U3T) and Lamin B (D9V6H) were provided by Cell Signaling Technology (Danvers, MA, USA). The primary antibody against Nrf2 (AF0639) was provided by Affinity Biosciences (Nanjing, China). The secondary antibodies were provided by Proteintech (Manchester, UK).

Cell culture and hypoxia model

Highly differentiated PC12 cells, obtained from Chinese Academy of Sciences Committee Type Culture Collection cell bank (Shanghai, China), were cultured in high-glucose DMEM (Bioss Biotechnologym Hangzhou, China) containing 10% FBS and 1% penicillin/streptomycin. PC12 cells were maintained at 37 °C in a humidified incubator supplied with 5% CO_2. The medium was refreshed every alternate day. PC12 cells in the logarithmic phase were incubated in a hypoxia condition containing 1% O_2, 5% CO_2, and 94% N_2 for 24 h to induce a hypoxia model.

Drug treatment and cell grouping

PC12 cells were plated onto 96-well plates at a density of 1×10^3 cells per well and incubated at 37 °C with 5% CO_2 for 24 h. In order to determine the optimal concentration of 6-OHG, cells were treated with various concentrations of 6-OHG (0, 0.004, 0.02, 0.10, 0.50 and 2.50 μM) or rutin (1.0 μM) for 2 h. Following that, PC12 cells were incubated under normoxia or hypoxia condition for 24 h. Next, to further investigate the protective effects of 6-OHG on hypoxia injury, PC12 cells were assigned to four groups: Normoxia (Nor) group, Hypoxia (Hy) group, Hy + rutin group and Hy + 6-OHG (5 μmol/L) group. To elucidate the role of Nrf2/HO-1 pathway in the protective effect of 6-OHG against hypoxia injury, PC12 cells were divided into four groups: Nor group, Hy group, Hy + 6-OHG group and Hy + 6-OHG + ML385 group (cells were treated with 0.5 μmol/L 6-OHG and 10 μM ML385 for 2 h, and then incubated in hypoxia conditions for 24 h). The concentration of ML385 was selected based on previous studies[17,18] and our preliminary experiment.

Cell viability assay

Cell viability was evaluated using CCK-8 assay. In brief, ten microliters of CCK-8 reagent (Bioss Biotechnology, Hangzhou, China) were added to each well and the mixtures were incubated at 37 °C for another 2 h. The optical density (OD) at 450 nm was measured using a microwell plate reader (Molecular Devices, Sunnyvale, USA). Cell viability was expressed as the percentage of normal cells.

Cell morphology and lactate dehydrogenase (LDH) release

The PC12 cells were inoculated into six-well culture plates at a density of 1×10^5 cells per well, and incubated in an incubator at 37 °C for 24 h. After treatment same as 2.2, the cell morphology was observed using ChemiDoc MP Imaging System (Bio-Rad). Then the cell culture medium was collected and centrifuged at 2500 r/min for 10 min obtain the supernatant. LDH levels in supernatant were determined using the commercial assay kit (Nanjing Jiancheng Bioengineering Research Institute, Nanjing, China) as per the manufacturer's protocol.

Calcein-AM/Propidium iodide (PI) staining assay

Calcein-AM/PI staining kits (Byotime Biotechnology Company, Hangzhou, China) was employed to detect the rates of live/dead cell. After stimulation as described above, the PC12 cells were collected and mixed with 1 mL Calcein AM solution, and then cultured for 0.5 h at 37 °C. Cells were rinsed twice with precooled PBS, and then stained with 4.5 μM PI for 5 min at 37 °C. A fluorescence microscope was used to capture the images. Red fluorescence and green fluorescence represented dead cells and live cells, respectively.

Reactive oxygen species (ROS) assay

Intracellular ROS levels were assessed using the DCFH-DA probe (Nanjing Jiancheng Bioengineering Research Institute, Nanjing, China). After stimulation as described above, the culture medium was removed, and then PC12 cells were incubated with 1 mL DCFH-DA solution (10 μM) for 20 min at 37 °C. After washing twice with precooled PBS, PC12 were observed under a fluorescence microscope. Percentage of positive cells were calculated from the captured images using image J software (version 8, National Institutes of Health).

Oxidative stress parameters assay

PC12 cells were inoculated at a density of 1×10^5 cells per well into six-well culture plates and treated as aforementioned. The PC12 cells were collected by centrifugation at 4 °C, 1500 r/min for 5 min. After washing with precooled PBS, cells were resuspended in 500 μL of lysis buffer and cracked on ice for 20 min. When completed, cell lysates were centrifuged at 4 °C, 12 000 g for 15 min to obtain the supernatant. The protein concentration was measured by BCA kit (Solarbio, Beijing, China). The levels of MDA, GSH, SOD and CAT were assessed using commercial assay kits (Nanjing Jiancheng Bioengineering Research Institute, Nanjing,

China) as per the manufacturer's protocol. The MDA and GSH results were expressed as nmol/mg protein. SOD and CAT activities were expressed as U/mg protein.

ELISA assay

After different stimulation as aforementioned, PC12 cells were collected. The contents of TNF-α, IL-6 and IL-10 in the cells were determined using commercial ELISA kits (Ruixin Biotechnolog company, Quanzhou, China) as per the manufacturer's protocol and expressed as pg/mg protein.

Caspase-3 and Caspase-9 activities assay

After different stimulation as aforementioned, PC12 cells were collected. Commercial kits (Nanjing Jiancheng Bioengineering Research Institute, Nanjing, China) were employed to determine caspase-3 and caspase-9 activities in cells as per the manufacturer's protocol. Samples were analyzed using a SpectraMax i3 plate reader (Molecular Devices, San Jose, CA, USA) at 405 nm, followed by fold change calculation.

Terminal deoxynucleotidyl transferase-mediated deoxy-UTP (dUTP) nick end labeling (TUNEL) staining assay

A TUNEL assay kit (Beyotime, Shanghai, China) was used to analyze apoptotic cells. PC12 cells in different groups were collected and then fixed with immunol staining fix solution for 30 min at 25 °C. Then, cells were washed with PBS and permeabilized with enhanced immunostaining permeabilization buffer for 5 min. Afterward, the cells were rinsed twice with PBS, and then 100 μL TUNEL solution were added to resuspend cells and maintained at 37 °C for 1 h in dark. After rinsing with PBS another three times, cells were analyzed using a fluorescence microscope. Percent positive cells were assessed by image J software (version 8, National Institutes of Health).

Immunofluorescence staining

PC12 cells were treated as aforementioned. The culture medium was discarded and cells in different groups were rinsed with PBS twice, fixed with immunol staining fix solution (P0098, Beyotime) for 20 min, and then permeabilised with enhanced immunostaining permeabilization buffer (P0097, Beyotime) for 30 min at 25 °C. Cells were blocked with 3% BSA for 30 min at 25 °C and incubated with primary antibody against Nrf2 and HO-1 for 12 h at 4 °C. Afterward, cells were incubated with the secondary antibody (Alexa Fluor 555 anti-rabbit IgG, 1:500, 4413 S; Cell Signaling Technology) in 37 °C water bath for 1 h away from light. Finally, DAPI was used stained nuclei for 5 min. After mounting with antifade mounting medium (Servicebio), cells were observed via a fluorescence microscope.

Western blot

PC12 cells in different groups were harvested and lysed by RIPA buffer containing 1% protease inhibitor cocktail (Meilunbio, Shanghai, China). Nuclear proteins were extracted using a nuclear and cytoplasmic protein extraction kit (P0028, Beyotime) as per the manufacturer's protocol. The protein concentration was quantified using the BCA kit. Equal quality of proteins was separated by sodium dodecyl sulfate–polyacrylamide gel electrophoresis (SDS-PAGE) gels and then transferred to polyvinylidene difluoride (PVDF) membranes (Millipore, MA, USA). The membranes were blocked with 5% non-fat milk at 25 °C for 2 h and then incubated with primary antibodies against HIF-1α (1:800), VEGF (1:1000), TNF-α (1:1000), NF-κB (1:1000), Bax (1:1000), Bcl-2 (1:1000), cleaved caspase-3 (1:1000), Nrf2 (1:1000), HO-1 (1:1000), β-actin (1:3000) and Lamin B (1:1000) overnight at 4 °C. Afterward, membranes were rinsed with Tris-buffered saline with Tween 20 (TBST).

three times and incubated with secondary antibody (1:10000) at 25 °C for 1 h. Finally, the membrane bands were visualized by the enhanced chemiluminescence (ECL) reagent under the Tanon 460SF Chemiluminescent Imaging System (Tanon Science & Techonlogy Co, Shanghai, China) and analyzed by Image J software (version 8, National Institutes of Health).

Molecular docking

The potential binding mode of 6-OHG to Nrf2 and HO-1 was investigated using Molecular docking analysis. The three-dimensional (3D) structure of 6-OHG was downloaded from PubChem (Compound CID: 5492944, https://pubchem.ncbi.nlm.nih.gov/). The structures of the Nrf2 (7K2F) and HO-1(3CZ1) were downloaded from the Protein Data Bank (PDB, http://www.rcsb.org)] and appropriately modified using Pymol software. Maestro 13.7 software was used to dock the 6-OHG to the receptor protein, and the docking results were visualized and analyzed by PyMOL software.

Statistical analysis

All data were analyzed using Prism software Version 8 (GraphPad, La Jolla, USA) and presented as a mean ± standard error of the mean (SEM). Differences were compared by one-way analyses of variance (ANOVA) corrected with Dunnett's test or Tukey's test when the data were normally distributed. p value less than 0.05 was considered as statistically significant.

Results

The integrated network pharmacology analysis indicated the potential targets mediated by 6-OHG in treating hypoxia injury

To predict the potential targets and pathways of 6-OHG against hypoxia injury, a network pharmacology approach was applied in the current study. As shown Figs. 1B and 534 potential targets of 6-OHG and 5847 hypoxia injury-associated targets were obtained, and 229 targets of 6-OHG interfering with hypoxia injury were

obtained through VENN screening. To explore the interactions in these genes, we constructed a PPI network, which consisted of 208 nodes and 699 edges. Notably, as seen from the PPI network (Fig. 1C and D), EGFR, HSP90AA1, HIF1A, ESR1, CCND1, PRKACA, MMP9 and NFKB1 were regarded as the corn targets for 6-OHG against hypoxia-induced injury.

To further explore the biological function of 6-OHG in the therapy of hypoxia-induced injury, functional and pathway enrichment analysis was performed in this study. 709 GO items were obtained by GO enrichment analysis, of which 466 were biological process (BP), 92 were cellular composition (CC), and 151 were molecular function (MF). As shown in Fig. 1E, BP was mainly associated with response to protein phosphorylation, negative regulation of apoptotic process and inflammatory response. The MF was associated with ATP binding, protein binding, protein kinase activity and enzyme binding. CC was mainly associated with nucleus, cytoplasm, nucleoplasm and mitochondrion. A total of 139 signaling pathways were obtained in the KEGG category. Notably, these signaling pathways related to oxidative stress, inflammatory response and apoptosis, such as MAPK signaling pathway, reactive oxygen species, p53 signaling pathway, HIF-1 signaling pathway and apoptosis, were highly enriched (Fig. 1F).

6-OHG attenuated hypoxia-stimulated injury in PC12 cells

The effect of 6-OHG at varying concentrations on the viability of PC12 cells was detected by CCK-8 assay. As seen in Figs. 2A and B and 3-OHG at doses from 0.004 μmol/L to 2.5 μmol/L had no significant toxicity on PC12 cells under normoxic condition. After 24 h of hypoxia exposure, PC12 cell viability remarkably reduced compared to the Nor group ($p < 0.01$), while treatment with 6-OHG at diverse doses from 0.004 μmol/L to 0.5 μmol/L elevated the cell viability ($p < 0.01$ or $p < 0.05$) in a dose dependent manner. When the concentration of 6-OHG reached 2.5 μmol/L, a small decrease in cell viability was observed, but it was still higher than that in the Hy group ($p < 0.05$). Thus, the subsequent experiments were performed at the concentration of 0.5 μmol/L.

We first analyzed the cellular morphology changes in PC12 cell. As seen in Fig. 2C, the cells in the Nor group grew well, with fusiform shape and clearly visible edges. The cells in the Hy group become round, and massive cells were shed and suspended in the culture medium. LDH is an indicator of cell membrane integrity and is released when the cell membrane is disrupted. As shown in Fig. 2D, compared to the Nor group, LDH content was remarkably increased in the supernatant of hypoxic PC12 cell. This effect was significantly inhibited by 6-OHG or rutin treatment, indicating that 6-OHG was able to preserve the integrity of the cell membrane. Moreover, we observed the survival status of the PC12 cell via Calcein-AM/PI staining. As shown in Fig. 2E, massive live cells (green fluorescence) and few dead cells (red fluorescence) were observed in the Nor group, whereas hypoxia stimulation induced more dead cells. 6-OHG was able to inhibit hypoxia-induced cells damage as evidence by the significant decreased number of dead cells. Thus, these findings demonstrate that 6-OHG can protective PC12 cells against hypoxia stimulated injury.

6-OHG inhibited hypoxia-stimulated oxidative stress in PC12 cells

Oxidative stress is critically associated with hypoxic injury[19]. Therefore, we investigated indicators of oxidative stress in hypoxic PC12 cells treated with 6-OHG. As seen in Fig. 3A-E, compared to the Nor group, hypoxia exposure significantly elevated the contents of cellular ROS and MDA, and decreased the activities of cellular SOD and CAT and the level of cellular GSH. 6-OHG treatment significantly reversed these changes. These results indicate that 6-OHG inhibits hypoxia-stimulated oxidative stress via removing excessive ROS, alleviating intracellular lipid peroxidation and increasing the antioxidant enzymes activities.

6-OHG regulated hypoxia-related factors in PC12 cells following hypoxia exposure

HIF-1α and its transcriptional target VEGF are two of main hypoxia-responsive genes[20]. Their expressions are regulated by oxygen concentration. As seen in Fig. 3F-H, compared to the Nor group, hypoxia stimulation significantly up-regulated the expressions of HIF-1α and VEGF proteins in PC12 cells ($p < 0.01$). However, 6-OHG treatment significantly down-regulated HIF-1α and VEGF protein expressions in hypoxic PC12 cells ($p < 0.01$), improving hypoxic status.

6-OHG inhibited hypoxia-stimulated inflammatory response in PC12 cells

Hypoxia-induced injury is also related to activation of the inflammatory response[21]. To assess whether 6-OHG could suppress hypoxia-induced inflammatory responses, we evaluated the levels of inflammatory factors in PC12 cells using ELISA kits and Western blotting. As seen in Fig. 4A-C, compared to the Nor group, the contents of pro-inflammatory cytokines TNF-α and IL-6 were significantly elevated, whereas the level of anti-inflammatory cytokine IL-10 was remarkably decreased in the hypoxia PC12 cells ($p < 0.01$). However, these effects were reversed by 6-OHG administration ($p < 0.01$). Western blot analysis indicated that hypoxia stimulation markedly increased the expressions of TNF-α and NF-κB in PC12 cell ($p < 0.01$). However, 6-OHG significantly reduced the increase in the expressions of TNF-α and NF-κB in PC12 cell (Fig. 4D-F). These results indicate that 6-OHG mitigates hypoxia damage on PC12 cells by suppressing inflammatory response.

6-OHG inhibited hypoxia-stimulated apoptosis in PC12 cells

Both hypoxia-induced oxidative stress and inflammatory responses can induce cell apoptosis. To evaluate whether 6-OHG protected PC12 cell against hypoxia-induced apoptosis, the number of apoptotic cells was analyzed by TUNEL staining. As seen in Fig. 5A, hypoxia stimulation significantly increased the number of apoptotic cells compared to the Nor group ($p < 0.01$). However, 6-OHG treatment remarkably decreased the number of the apoptotic cells. Given that caspases are key regulators of cell apoptosis[22], the activities of caspase-3 and −9 were assessed. As shown in Fig. 5B-C, compared to the Nor group, the activities of caspase-3 and −9 were significantly enhanced in PC12 cell under hypoxia conditions, whereas 6-OHG treatment significantly decreased

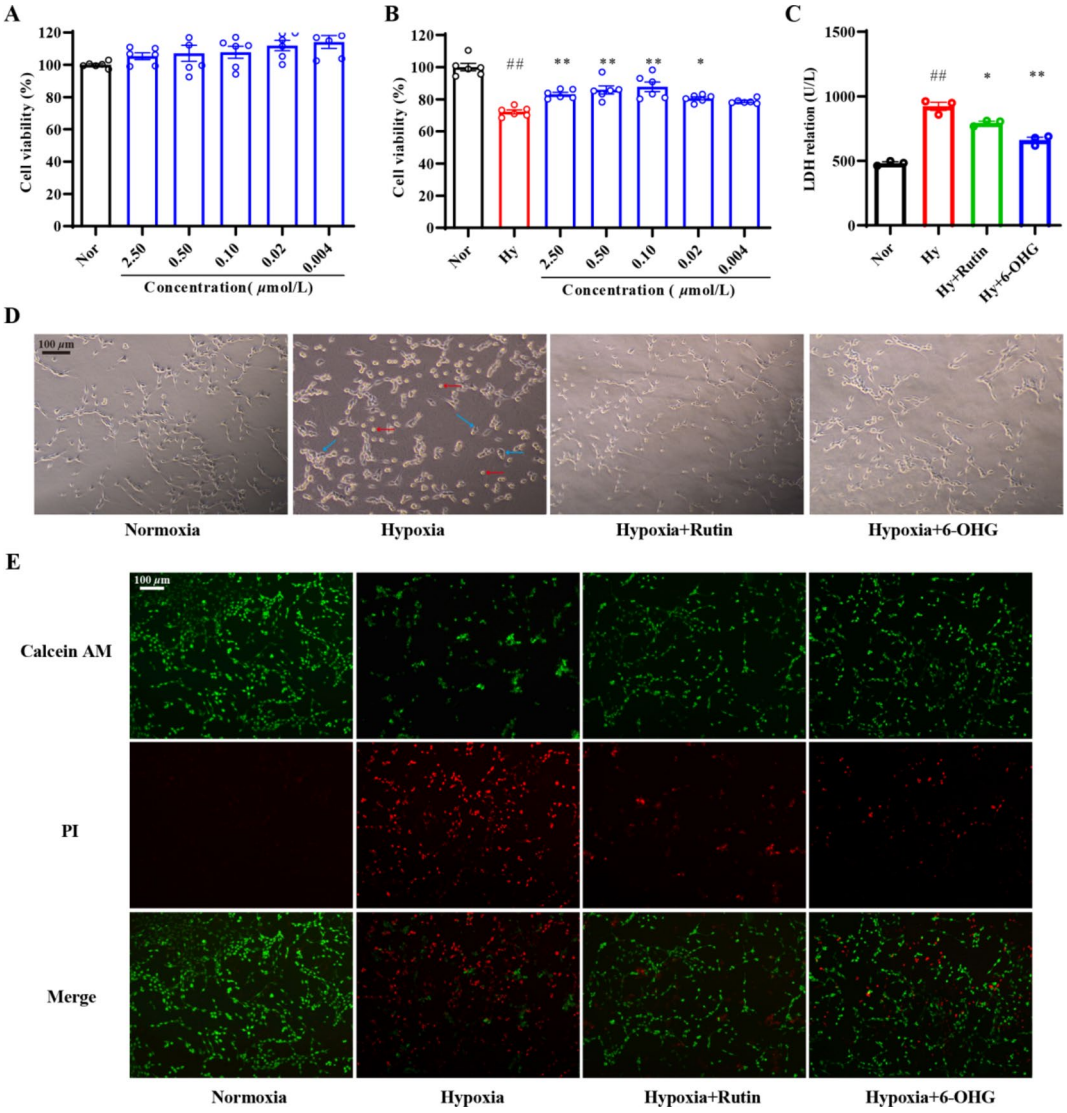

Fig. 2. 6-OHG attenuated hypoxia-stimulated injury in PC12 cells. (**A**) Effect of 6-OHG on cell viability in PC12 cells under normal condition, (**B**) Effect of 6-OHG on cell viability in PC12 cells under hypoxia condition, (**C**) LDH release from PC12 cells, (**D**) Cell morphology was viewed under the light microscope, red arrow: round and floating cells, blue arrow: wrinkled cell. (**E**) Living and dead cells were detected by calcein-AM/PI staining and then visualized by fluorescence microscopy (magnification, ×200). The cells stained with green were living cells, and those stained with red were dead cells. Data are expressed as mean ± SEM ($n = 6$ or 3). Statistical analysis was performed using one-way ANOVA corrected with Dunnett's test (A, B) or Tukey's test (C). $^{\#}p < 0.05$ or $^{\#\#}p < 0.01$ versus Nor group; $^{*}p < 0.05$ or $^{**}p < 0.01$ versus Hy group.

the activities of caspase-3 and −9 in hypoxia PC12 cells. Bax acts in the upstream pathway of caspases, leading to the release of cytochrome c from mitochondria, which in turn activates caspase. As shown by western blot assay (Fig. 5D-F), hypoxia stimulation significantly up-regulated the protein levels of Bax and cleaved caspase-3 and the ratio of Bax/Bcl-2, whereas down-regulated the protein level of Bcl-2 ($p < 0.01$) in PC12 cells compared with Nor group. However, 6-OHG treatment could reverse these changes. Together, these data indicate that 6-OHG suppresses hypoxia induced apoptosis.

6-OHG activated the Nrf2/HO-1 signaling pathway in PC12 cells following hypoxia exposure

To explore whether the Nrf2/HO-1 signaling pathway is engaged in the protective effect of 6-OHG against hypoxia injury, the expressions of Nrf2 and HO-1 were analyzed using western blot and immunofluorescence staining. As seen in Fig. 6A-C, hypoxia stimulation significantly inhibited Nrf2 nuclear translocation and the expression of HO-1 ($p < 0.01$), indicating that the Nrf2/HO-1signaling pathway was inhibited. 6-OHG treatment significantly reversed these changes. The results of immunofluorescence staining (Fig. 6D-F) were consistent with the above results, indicating that 6-OHG may activate the Nrf2/HO-1 signaling pathway to exert protective role in PC12 cells following hypoxia exposure.

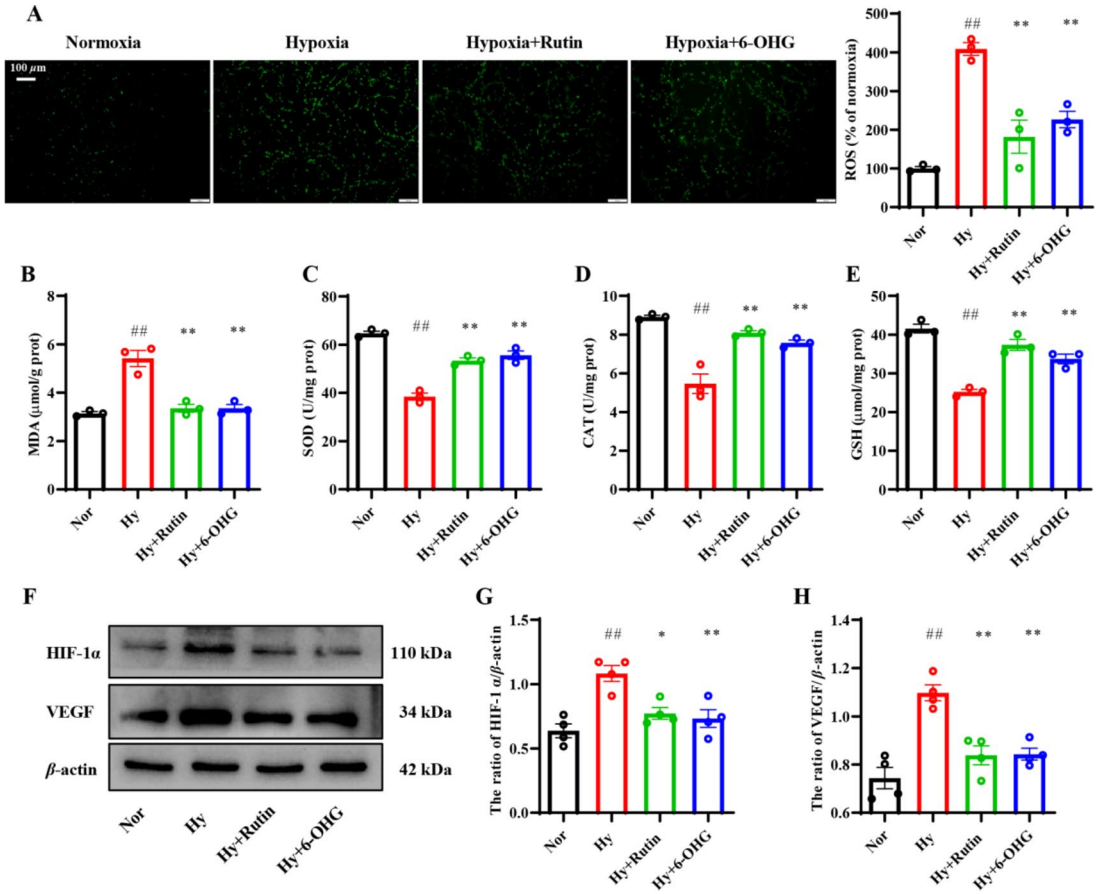

Fig. 3. 6-OHG inhibited hypoxia-stimulated oxidative stress in PC12 cells. (**A**) The ROS level measured by DCFH-DA on a fluorescence microscope. MDA content (**B**), SOD activity (**C**), CAT activity (**D**), and GSH level (**E**) in the cell lysis supernatant were determined by corresponding kits. (**F**) The protein expression levels of HIF-1a and VEGF were detected by Western blotting. (B) Quantitative analysis of the expression of HIF-1a (**G**) and VEGF (**H**) proteins. Data are expressed as mean ± SEM (n = 3 or 4). Statistical analysis was performed using one-way ANOVA corrected with Tukey's test. $^{\#}p < 0.05$ or $^{\#\#}p < 0.01$ versus Nor group; $^{*}p < 0.05$ or $^{**}p < 0.01$ versus Hy group.

Molecular docking

To verified the potential targets of 6-OHG against hypoxia-induced injury, we conducted molecular docking analysis. As illustrated in Fig. 6G and H, amino acid residues SER602, SER363 and ARG380 in the Nrf2 protein and amino acid residues PH3117 and TRP116 in the HO-1 protein can interact with 6-OHG. The docking score of 6-OHG with Nrf2 and HO-1 were calculated to be −4.744 and − 5.463 with free binding energies of −47.40 and − 25.54 kcal/mol, respectively. The low binding free energy indicates that 6-OHG owns strong binding stability with Nrf2 and HO-1.

ML385 reversed the effect of 6-OHG on proliferation vitality and activation of Nrf2/HO-1 signaling pathway in PC12 cells exposed to hypoxia

To elucidate the mechanism underlying the protective effect of 6-OHG against hypoxia injury via the Nrf2/HO-1 pathway, we investigated the impact of ML385, a specific inhibitor of the Nrf2, on PC12 cells treated with 6-OHG under hypoxia condition. As seen in Fig. 7A-C, compared to the Hy group, 6-OHG treatment remarkably increased cell viability, decreased the LDH release and the numbers of dead cell. As expected, the beneficial effects of 6-OHG against hypoxia injury was counteracted by ML385. Furthermore, we measured the key markers of Nrf2/HO-1signaling pathway by western blotting and immunofluorescence staining. 6-OHG treatment significantly increased Nrf2 nuclear translocation and the expression of HO-1 compared to the Hy group. However, treatment with ML385 significantly reversed these changes (Fig. 7D-F). Similar results were also obtained by Immunofluorescence staining (Fig. 7G-I). These results indicate that ML385 significantly inhibits the activation of Nrf2/HO-1 signaling pathway by 6-OHG in hypoxic PC12 cells.

ML385 counteracted the inhibitory effect of 6-OHG on hypoxia-stimulated oxidative stress, inflammatory response and apoptosis in PC12 cells

We also confirmed that ML385 treatment counteracted the effects of 6-OHG on the reduction of ROS and MDA, as well as the elevation of SOD and GSH in PC12 cells exposed to hypoxia ($p < 0.05$) (Fig. 8A-D). In addition,

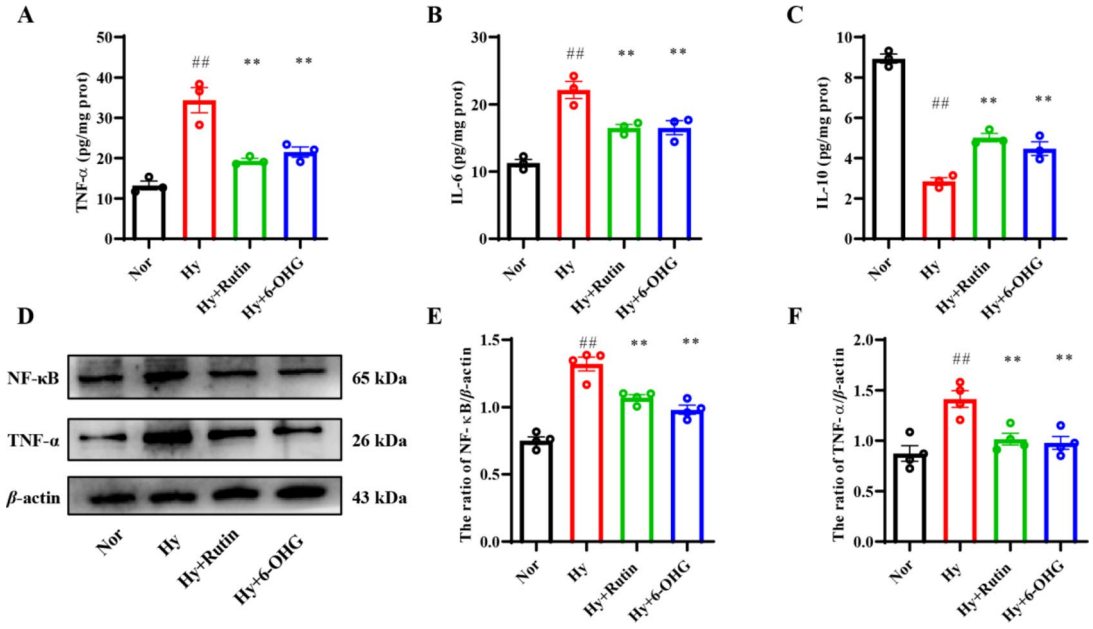

Fig. 4. 6-OHG inhibited hypoxia-stimulated inflammatory response in PC12 cells. The levels of TNF-a (**A**), IL-6 (**B**) and IL-10 (**C**) in the cell lysis supernatant were analyzed by ELISA. (**D**) The protein expression levels of TNF-a and NF-kB were detected by Western blotting. Quantitative analysis of the expression of TNF-a (**E**) and NF-kB (**F**) proteins. Data are expressed as mean ± SEM (n = 3 or 4). Statistical analysis was performed using one-way ANOVA corrected with Tukey's test. $^{\#}p < 0.05$ or $^{\#\#}p < 0.01$ versus Nor group; $^{*}p < 0.05$ or $^{**}p < 0.01$ versus Hy group.

ML385 greatly upregulated the protein levels of TNF-α and NF-κB ($p < 0.05$) (Fig. 8E-G) and counteracted the ameliorative effect of 6-OHG on hypoxia-induced inflammatory response. Finally, ML385 treatment offset the inhibitory effect of 6-OHG against apoptosis induced by hypoxia ($p < 0.01$ or $p < 0.05$) (Fig. 8H-K).

Dissusion

Hypoxia is an important stressor that induces cellular damage, and the central nervous system is highly sensitive to hypoxic stress[23]. However, effective preventive and therapeutic drugs are still lacking. This study verified for the first time the protective mechanism of 6-OHG against damage caused by hypoxia via network pharmacology and cellular experiments in vitro, which was related to attenuate oxidative stress and inflammatory response, as well as suppress apoptosis via activation of Nrf2/HO-1 signaling pathway.

We first systematically analyzed the possible mechanisms of action of 6-OHG in ameliorating hypoxia injury using a network pharmacology approach. The results indicated that 229 potential therapeutic targets of 6-OHG for the treatment of hypoxia injury were identified, among which EGFR, HSP90AA1, HIF1A, ESR1, MMP9 and NFKB1 were the core targets. Subsequent PPI network, GO and KEGG enrichment analysis demonstrated that 6-OHG might be effective in the treatment of hypoxia injury by regulating hypoxia-induced oxidative stress, inflammatory response and apoptosis.

In vitro study, we clarified that after 6-OHG intervention, hypoxia-induced changes in cell morphology, reduction in cell viability, and damage to cell membrane integrity were all ameliorated, which effectively attenuated the injury caused by hypoxia in PC12 cells. In addition, hypoxia induces intense oxidative stress along with a decrease in the activity of antioxidant enzymes and excessive generation of ROS[24], which attacks cellular proteins, lipids, DNA and other biological molecules, ultimately triggering injury[25]. MDA is the end product of lipid peroxidation and can reflect the severity of cellular exposure to free radicals. SOD, CAT and GSH-Px are important antioxidant enzymes for cells to fight against oxidative stress damage, and their activities reflect the body's ability to scavenge excess ROS[26]. In the current study, hypoxia stimulation greatly elevated the contents of ROS and MDA, but significantly reduced the SOD and CAT activities, and GSH content in PC12 cells. While 6-OHG treatment remarkably inhibited oxidative stress by reducing ROS and MDA levels, and enhancing GSH level as well as SOD and CAT activities.

HIF-1α is a critical oxygen-regulated transcriptional activator that regulates cellular adaptive responses to hypoxia[27]. Up-regulation of HIF-1α can promote cell survival under hypoxia by inducing the transcription of hypoxia-related genes[28], but HIF-1α has also been implicated as a marker of intracellular hypoxia[29]. In addition, ROS can enhance HIF-1α expression by inhibiting PHD function[30]. Therefore, high expression of HIF-1α also reflects the oxidative stress status of the cells[31,32]. Our findings supported that 6-OHG treatment inhibited hypoxia-induced increases in expressions of HIF-1α and VEFG, suggesting that resistance to oxidative stress injury induced by hypoxia might be one of the protective mechanisms of 6-OHG.

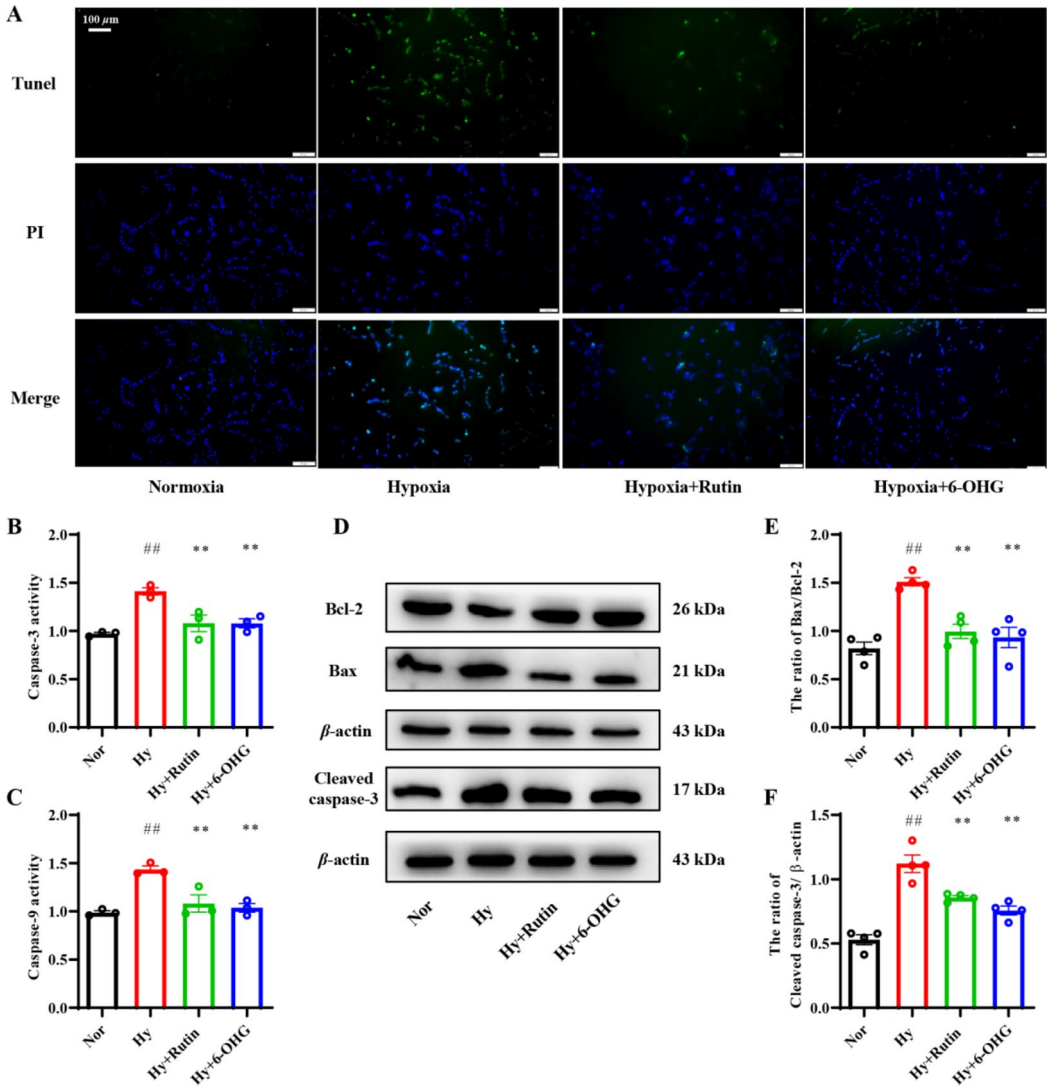

Fig. 5. 6-OHG inhibited hypoxia-stimulated apoptosis in PC12 cells. (**A**) The apoptosis of PC12 cells was detected by TUNEL staining (Magnification, × 20). The activities of Caspase-3 (**B**) and Caspase-9 (**C**) was measured by corresponding kits. (**D**) The protein expression levels of Bax, Bcl-2 and cleaved caspase-3 were detected by Western blotting. Quantitative analysis of the ratio of Bax/Bcl-2 (**E**) and the expression of cleaved caspase-3 (**F**) protein level. Data are expressed as mean ± SEM (n = 3 or 4). Statistical analysis was performed using one-way ANOVA corrected with Tukey's test. $^{\#}p < 0.05$ or $^{\#\#}p < 0.01$ versus Nor group; $^{*}p < 0.05$ or $^{**}p < 0.01$ versus Hy group.

Inflammatory response, characterized by increased expression of pro-inflammatory cytokines, including IL-1β, IL-6, and TNF-α, has been demonstrated under hypoxic conditions[33]. Consistent with the previous results, we also found that the levels of pro-inflammatory cytokines IL-6 and TNF-α significantly enhanced, and the level of anti-inflammatory cytokine IL-10 significantly reduced in PC12 cell following hypoxia stimulation. While 6-OHG treatment reverse the corresponding trend of change. NF-κB is a key transcription factor that mediates the inflammatory response by regulating the release of inflammatory cytokines[34]. TNF-α is one of the target genes of NF-κB activation, which can regulate NF-κB activity by inhibiting or enhancing the downstream pathway[35]. In the current study, the expressions of NF-κB and TNF-α in hypoxic PC12 cells were significantly increased. While 6-OHG treatment significantly downregulated the expressions of NF-κB and TNF-α. These results suggest that 6-OHG mitigates hypoxia induced inflammatory response through suppressing the NF-κB activation.

Studies have shown that apoptosis induced by oxidative stress and inflammatory responses was also contributed to the hypoxic injury[36]. The results of TUNEL staining in this study also indicated that 6-OHG treatment remarkably inhibited hypoxia induced cell apoptotic. Apoptosis is a type of programmed cell death that usually occurs through intrinsic or extrinsic pathways. The intrinsic apoptotic pathway is regulated by members of the pro-apoptotic b-cell lymphoma-2 (Bcl-2) family, which consists mainly of pro-apoptotic proteins, such as the Bcl-2-associated X protein (Bax) and the Bcl-2 antagonist/killer protein (Bak) as well as anti-apoptotic

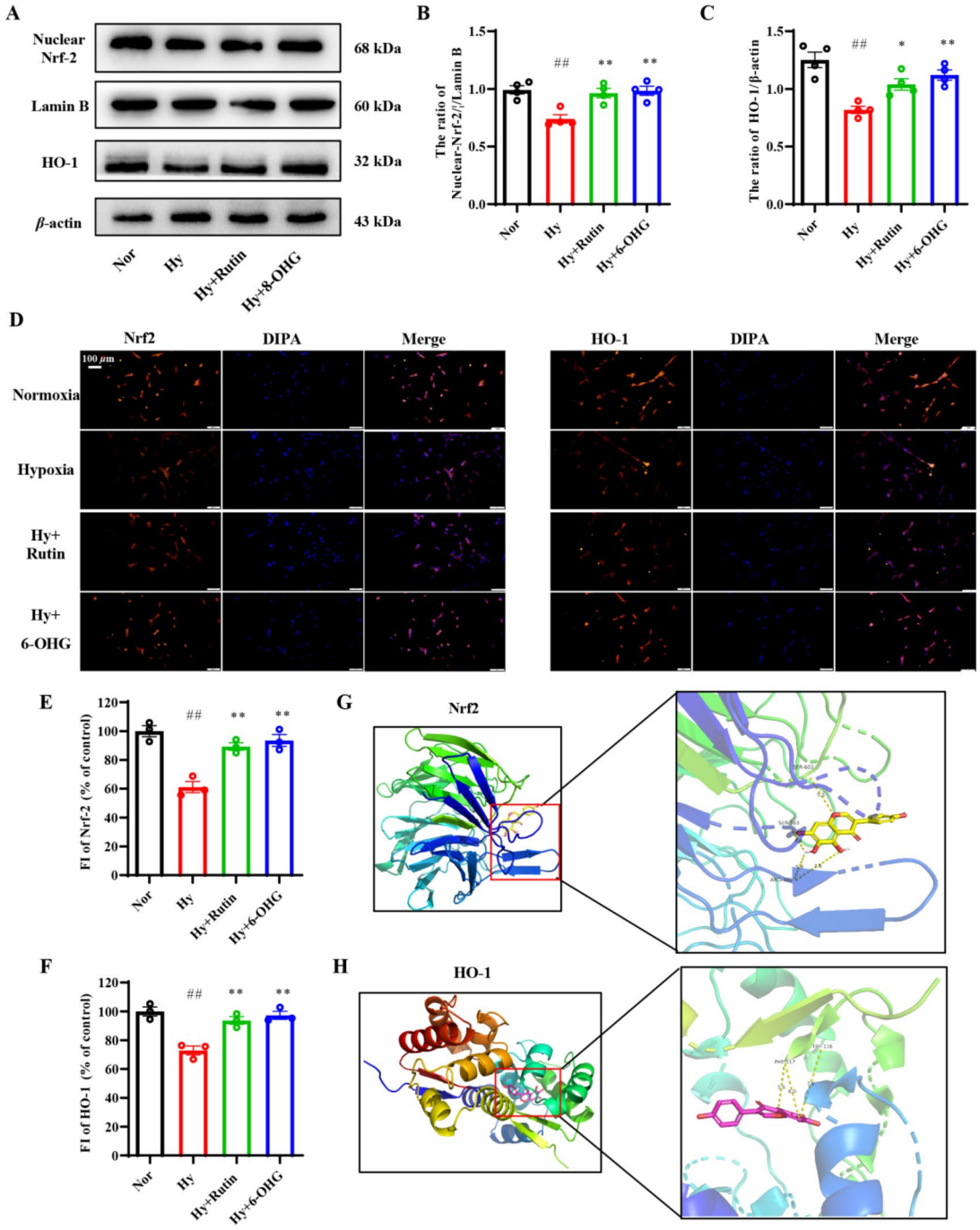

Fig. 6. 6-OHG activated the Nrf2/HO-1 signaling pathway in PC12 cells following hypoxia exposure (**A**) The protein expression levels of Nrf2 and HO-1 were detected by Western blotting. (**B**) Quantitative analysis of the expression of Nrf2 in nucleus (**C**) an HO-1(**D**). (**E**) The protein levels of Nrf2 and HO-1 were detected by Immunofluorescence staining. (**F**) Quantitative analysis of the fluorescence intensity of Nrf2 and HO-1. Molecular docking of 6-OHG binding to the targets. (**G**) Nrf2 (free binding energy,−47.40 kcal/mol). (**H**) HO-1 (free binding energy, −25.54 kcal/mol). Data are expressed as mean ± SEM (n = 3 or 4). Statistical analysis was performed using one-way ANOVA corrected with Tukey's test. $^{\#}p < 0.05$ or $^{\#\#}p < 0.01$ versus Nor group; $^{*}p < 0.05$ or $^{**}p < 0.01$ versus Hy group.

proteins such as Bcl-2 and Mcl-1[37]. Caspases are apoptosis executors[38]. In particular, cleaved caspase-3 triggers downstream protein phosphorylation, leading to membrane vesicles and cell shrinkage and amplifies apoptotic signals by activating other pre-caspases through protein hydrolysis. Therefore, regulating the expression of Bcl-2 family proteins and Cleaved caspase-3 is an important strategy to prevent apoptosis. In the present study, hypoxia exposure resulted in a significant increase in the activities of caspase-3 and −9 and the levels of pro-apoptotic proteins cleaved caspase-3 and Bax, concomitant with decrease in the level of anti-apoptotic protein

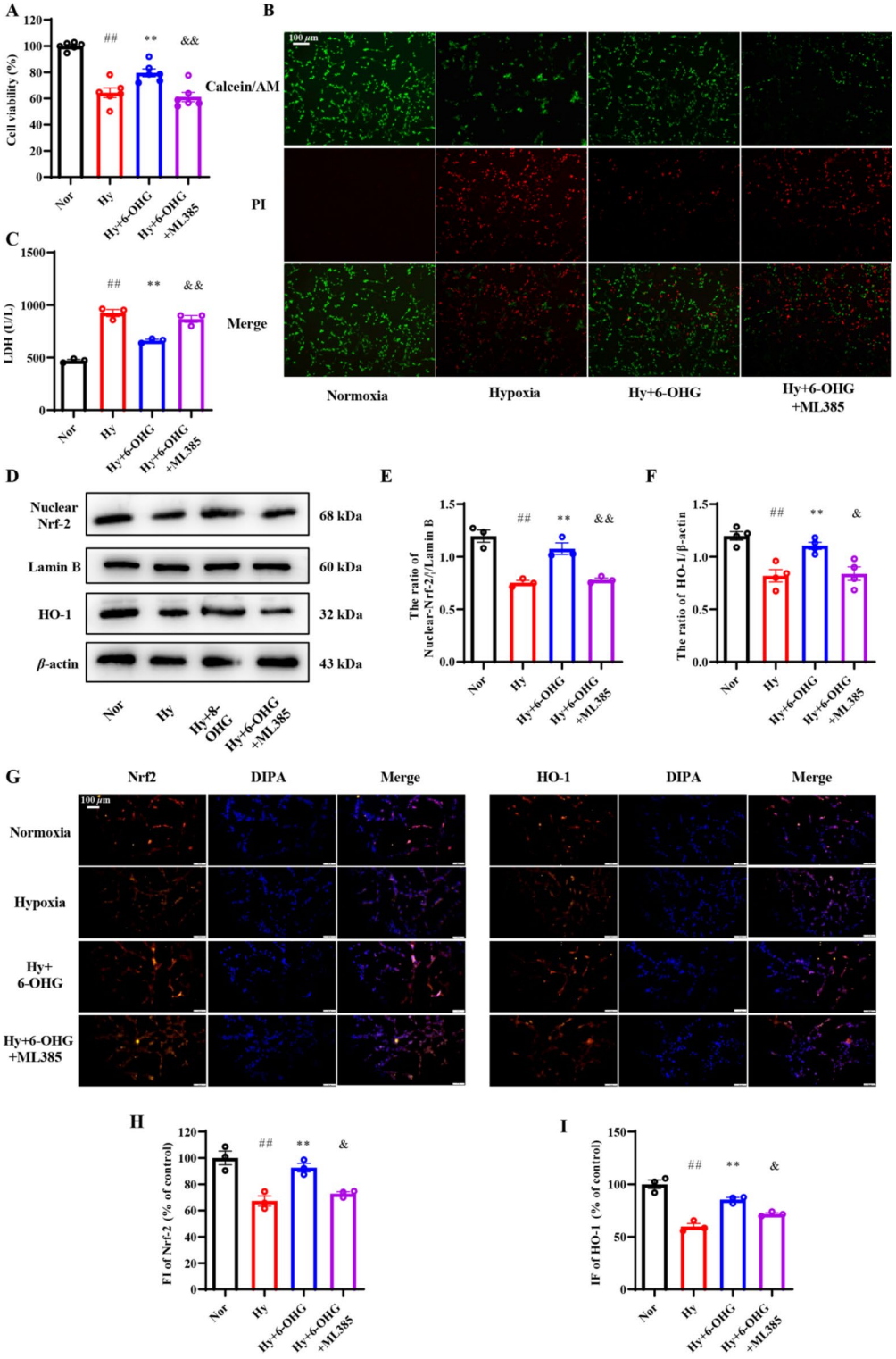

Fig. 7. ML385 reversed the effect of 6-OHG on proliferation vitality and activation of Nrf2/HO-1 signaling pathway in hypoxia-stimulated PC12 cells. (**A**) Cell viability assay (**B**) Calcein-AM/PI staining assays, (**C**) LDH leakage assay, (**D**) The protein expression levels of Nrf2 and HO-1 were detected by Western blotting. Quantitative analysis of the expression of Nrf2 in nucleus (**E**) and HO-1 (**F**). (**G**) The protein levels of Nrf2 and HO-1 were detected by Immunofluorescence staining. Quantitative analysis of the fluorescence intensity of Nrf2 (**H**) and HO-1 (**I**). Data are expressed as mean ± SEM (n = 3 or 4). Statistical analysis was performed using one-way ANOVA corrected with Tukey's test. $^{\#}p < 0.05$ or $^{\#\#}p < 0.01$ versus Nor group; $^{*}p < 0.05$ or $^{**}p < 0.01$ versus Hy group. $^{\&}p < 0.05$ or $^{\&\&}p < 0.01$ versus Hy + 6-OHG group.

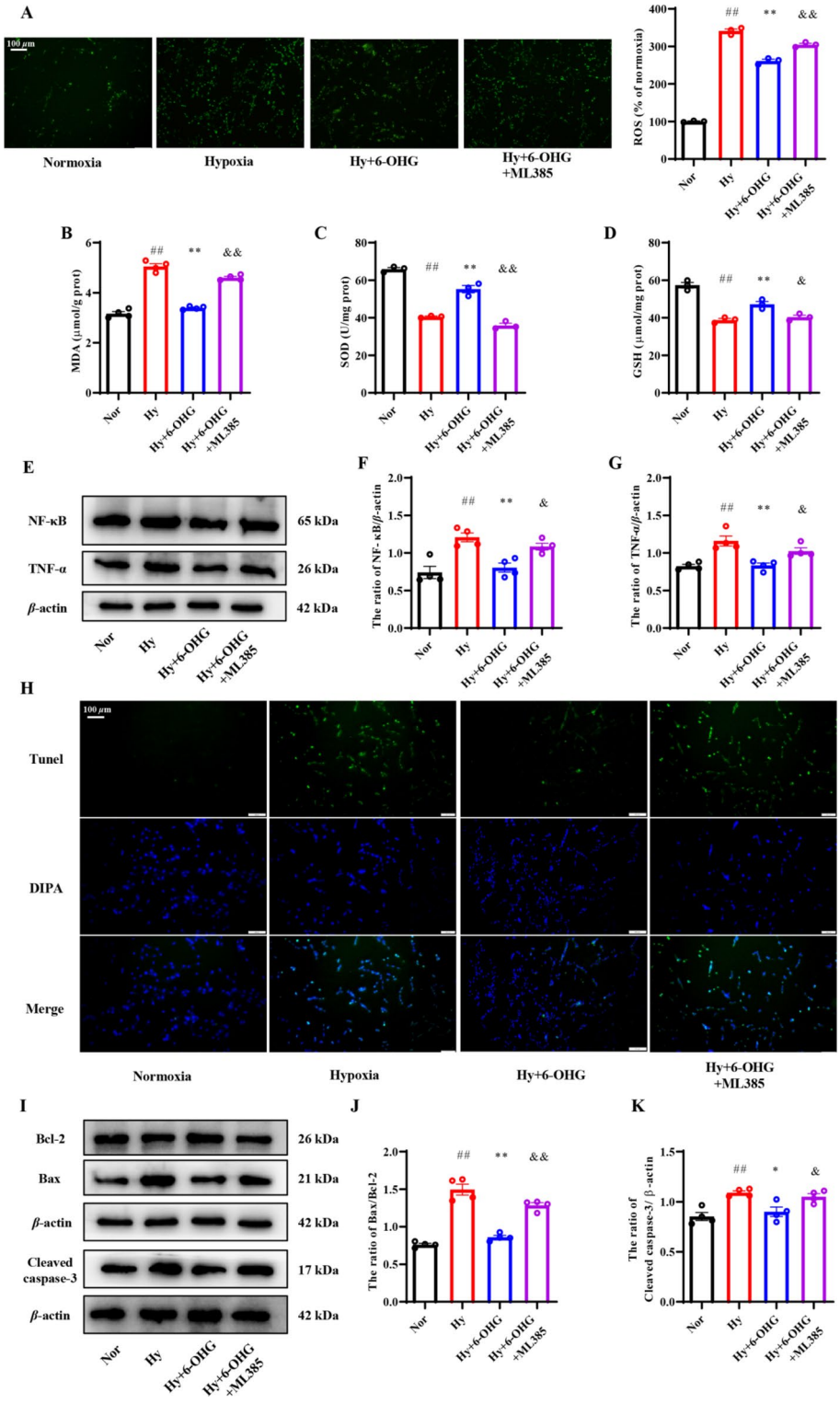

Fig. 8. ML385 counteracted the inhibitory effect of 6-OHG on hypoxia-stimulated oxidative stress, inflammatory response and apoptosis in PC12 cells. (**A**) The ROS level measured by DCFH-DA on a fluorescence microscope. MDA content (**B**), SOD activity (**C**), and GSH level (**D**) in the cell lysis supernatant were determined by corresponding kits. (**E**) The protein expression levels of TNF-a and NF-kB were detected by Western blotting. Quantitative analysis of the expression of TNF-a (**F**) and NF-kB (**G**). (**H**) The apoptosis of PC12 cells was measured by flow cytometry, Percentage of apoptotic cells were counted. (**I**) The apoptosis of PC12 cells was detected by TUNEL staining (Magnification, × 20). (**J**) The protein expression levels of Bax/Bcl-2 (**K**) and cleaved caspase-3 (L) were detected by Western blotting. Quantitative analysis of the ratio of Bax/Bcl-2 and the expression of cleaved caspase-3 protein level. Data are expressed as mean ± SEM (n = 3 or 4). Statistical analysis was performed using one-way ANOVA corrected with Tukey's test $^{\#}p < 0.05$ or $^{\#\#}p < 0.01$ versus Nor group; $^{*}p < 0.05$ or $^{**}p < 0.01$ versus Hy group. $^{\&}p < 0.05$ or $^{\&\&}p < 0.01$ versus Hy + 6-OHG group.

Bcl-2 in PC12 cells. 6-OHG treatment significant reversed these changes. These data suggest that the protective effect of 6-OHG on hypoxia induced damage was associated with its alleviative effect on apoptosis.

When cells are exposed to stressors such as oxidative stress and inflammation, Nrf2 is isolated from Keap1, then translocated and enriched in the nucleus, which in turn regulates the expression of a series of downstream antioxidant factors, including HO-1, NAD(P)H quinone oxidoreductase (NQO1), SOD, GSH-Px and etc., by binding to the antioxidant response elements (AREs). HO-1 is an important stress-inducible enzyme that catalytically decomposes hemoglobin into CO, $Fe^{2+}$and biliverdin, which can be further reduced to bilirubin, thus exerting antioxidant, anti-inflammatory and anti-apoptotic effects[39]. Therefore, the Nrf2/HO-1 signaling pathway plays an important role in maintaining cellular homeostasis under stress. Previous studies have proved that hypoxia inhibited Nrf2/HO-1 pathway[40,41]and activation of the Nrf2/HO-1 pathway may be effective for the treatment of hypoxia injury[42,43]. Also, several natural isoflavones with similar structure with 6-OHG have been identified as Nrf2 inducers, including daidzein[44], genistein[45], calycosin[46], biochanin A[47]. Theses above researches suggest that the Nrf2/HO-1 pathway may be involved in the beneficial effects of 6-OHG on hypoxic injury. As expect, our study confirmed that 6-OHG significantly increased the Nrf2 nuclear translocation and the expression of HO-1 in hypoxia-stimulated PC12 cells. These findings were also consistent with the results obtained from immunofluorescence staining. In addition, we docked Nrf2 and HO-1 with 6-OHG using molecular docking. The binding free energy was lower than −30 kcal/mol, suggesting that both Nrf2 and HO-1 had strong binding ability with 6-OHG. Moreover, ML385, a known inhibitor of Nrf2, partially abolished the mitigation effect of 6-OHG against oxidative stress, inflammatory response, and apoptosis induced by hypoxia in PC12 cells. These above results indicate that 6-OHG protects the PC12 cell against hypoxic injury via activating of the Nfr2/HO-1 pathway.

In summary, we have demonstrated that 6-OHG exhibits significant protective effects against hypoxia-induced PC12 cell damage. These beneficial effects appear to be achieved through activation of the Nrf2/HO-1 signaling pathway, which attenuates oxidative stress, inflammatory responses and apoptosis. In light of these findings, 6-OHG is a promising agent for the treatment of hypoxic nerve injury. Future investigations will be done to verify the results through animal experiments. Additionally, highly efficient formulations of 6-OHG also need to be developed for enhancing its solubility and bioavailability, which is beneficial for its further clinical application. This study also has certain limitations. First, we chose the optimal dose of 6-OHG to study its protective effect on hypoxic injury, that ignored the investigation of the dose dependence. In the future, we will set up different concentrations in animal experiments to investigate the dose dependence. Second, molecular docking suggested that 6-OHG could interact with Nrf2 and HO-1 proteins, but further experimental studies are needed to confirm this finding. Finally, given the complexity of the action mechanism of natural products and the results of network pharmacology analysis, whether 6-OHG can reduce hypoxia injury through other pathways, such as PI3K/AKT signaling pathway, also needs to be further assessed.

Data availability

All data generated or analysed during this study are included in this published article and its Supplementary Information files.

Received: 31 July 2024; Accepted: 1 January 2025
Published online: 06 January 2025

References

1. Marmura, M. J. & Hernandez, P. B. High-altitude headache. *Curr. Pain Headache Rep.* **19**, 483. https:/ (2015).
2. Li, B. et al. Inhibition of RhoA/ROCK pathway in the early stage of Hypoxia ameliorates Depression in mice via protecting myelin sheath. *ACS Chem. Neurosci.* **11**, 2705–2716. https://doi.org/10.1021/acschemneuro.0c00352 (2020).
3. Adingupu, D. D., Soroush, A., Hansen, A., Twomey, R. & Dunn, J. F. Brain hypoxia, neurocognitive impairment, and quality of life in people post-COVID-19. *J. Neurol.* **270**, 3303–3314. https://doi.org/10.1007/s00415-023-11767-2 (2023).
4. Jing, L. et al. Norwogonin attenuates hypoxia-induced oxidative stress and apoptosis in PC12 cells. *BMC Complement. Med. Ther.* **21**, 18. https://doi.org/10.1186/s12906-020-03189-8 (2021).
5. Kim, S. R., Seong, K. J., Kim, W. J. & Jung, J. Y. Epigallocatechin Gallate protects against Hypoxia-Induced inflammation in Microglia via NF-κB suppression and Nrf-2/HO-1 activation. *Int. J. Mol. Sci.* 23. https://doi.org/10.3390/ijms23074004 (2022).
6. Cheng, S., Chen, C. & Wang, L. Gelsemine exerts neuroprotective effects on neonatal mice with hypoxic-ischemic brain Injury by suppressing inflammation and oxidative stress via Nrf2/HO-1 pathway. *Neurochem Res.* **48**, 1305–1319. https://doi.org/10.1007/s11064-022-03815-6 (2023).
7. Chang, T. S. Isolation, bioactivity, and production of Ortho-Hydroxydaidzein and Ortho-Hydroxygenistein. *Int. J. Mol. Sci.* **15**, 5699–5716. https://doi.org/10.3390/ijms15045699 (2014).
8. Liu, L. et al. Traditional fermented soybean products: processing, flavor formation, nutritional and biological activities. *Crit. Rev. Food Sci. Nutr.* **62**, 1971–1989. https://doi.org/10.1080/10408398.2020.1848792 (2022).
9. Shao, J., Zhao, T., Ma, H. P., Jia, Z. P. & Jing, L. L. Synthesis, characterization, and Antiradical Activity of 6-Hydroxygenistein. *Chem. Nat. Compd.* **56**, 821–826. https://doi.org/10.1007/s10600-020-03161-5 (2020).
10. Chang, T. S., Ding, H. Y., Tai, S. S. K. & Wu, C. Y. Mushroom tyrosinase inhibitory effects of isoflavones isolated from soygerm koji fermented with aspergillus oryzae BCRC 32288. *Food Chem.* **105**, 1430–1438. https://doi.org/10.1016/j.foodchem.2007.05.019 (2007).
11. Chen, Y. C., Inaba, M., Abe, N. & Hirota, A. Antimutagenic activity of 8-hydroxyisoflavones and 6-hydroxydaidzein from soybean miso. *Biosci. Biotechnol. Biochem.* **67**, 903–906. https://doi.org/10.1271/bbb.67.903 (2003).
12. Tsuchihashi, R. et al. Microbial transformation and bioactivation of isoflavones from Pueraria flowers by human intestinal bacterial strains. *J. Nat. Med.* **63**, 254–260. https://doi.org/10.1007/s11418-009-0322-z (2009).
13. Hao da, C. & Xiao, P. G. Network pharmacology: a Rosetta Stone for traditional Chinese medicine. *Drug Dev. Res.* **75**, 299–312. https://doi.org/10.1002/ddr.21214 (2014).
14. Wiatrak, B., Kubis-Kubiak, A., Piwowar, A. & Barg, E. PC12 cell line: cell types, Coating of Culture vessels, differentiation and other Culture conditions. *Cells* **9** https://doi.org/10.3390/cells9040958 (2020).

15. Kanehisa, M. & Goto, S. KEGG: kyoto encyclopedia of genes and genomes. *Nucleic Acids Res.* **28**, 27–30. https://doi.org/10.1093/nar/28.1.27 (2000).
16. Sundaram, R. L., Sali, V. K. & Vasanthi, H. R. Protective effect of rutin isolated from Spermococe hispida against cobalt chloride-induced hypoxic injury in H9c2 cells by inhibiting oxidative stress and inducing apoptosis. *Phytomedicine* **51**, 196–204. https://doi.org/10.1016/j.phymed.2018.09.229 (2018).
17. Guo, L. T. et al. Baicalin ameliorates neuroinflammation-induced depressive-like behavior through inhibition of toll-like receptor 4 expression via the PI3K/AKT/FoxO1 pathway. *J. Neuroinflammation.* **16**, 95. https://doi.org/10.1186/s12974-019-1474-8 (2019).
18. Kang, J. et al. N-acetylserotonin protects PC12 cells from hydrogen peroxide induced damage through ROS mediated PI3K/AKT pathway. *Cell. Cycle.* **21**, 2268–2282. https://doi.org/10.1080/15384101.2022.2092817 (2022).
19. Auti, A. et al. Protective effect of Resveratrol against Hypoxia-Induced neural oxidative stress. *J. Pers. Med.* **12** https://doi.org/10.3390/jpm12081202 (2022).
20. Tirpe, A. A., Gulei, D., Ciortea, S. M., Crivii, C. & Berindan-Neagoe, I. Hypoxia: overview on hypoxia-mediated mechanisms with a focus on the role of HIF genes. *Int. J. Mol. Sci.* **20**, 6140. https://doi.org/10.3390/ijms20246140 (2019).
21. Eltzschig, H. K. & Carmeliet, P. Hypoxia and inflammation. *N Engl. J. Med.* **364**, 656–665. https://doi.org/10.1056/NEJMra0910283 (2011).
22. Sahoo, G., Samal, D., Khandayataray, P. & Murthy, M. K. A review on caspases: key regulators of Biological activities and apoptosis. *Mol. Neurobiol.* **60**, 5805–5837. https://doi.org/10.1007/s12035-023-03433-5 (2023).
23. LaManna, J. C. Hypoxia in the central nervous system. *Essays Biochem.* **43**, 139–151. https://doi.org/10.1042/bse0430139 (2007).
24. Cuenca, N. et al. Cellular responses following retinal injuries and therapeutic approaches for neurodegenerative diseases. *Prog Retin Eye Res.* **43**, 17–75. https://doi.org/10.1016/j.preteyeres.2014.07.001 (2014).
25. Sahu, B. et al. Oxidative stress resistance 1 gene therapy retards neurodegeneration in the rd1 mutant mouse model of Retinopathy. *Invest. Ophthalmol. Vis. Sci.* **62**, 8. https://doi.org/10.1167/iovs.62.12.8 (2021).
26. Guo, Y. et al. Antioxidant and immunomodulatory activity of selenium exopolysaccharide produced by Lactococcus lactis subsp. lactis. *Food Chem.* **138**, 84–89. https://doi.org/10.1016/j.foodchem.2012.10.029 (2013).
27. Semenza, G. L. HIF-1 and mechanisms of hypoxia sensing. *Curr. Opin. Cell. Biol.* **13**, 167–171. https://doi.org/10.1016/s0955-0674(00)00194-0 (2001).
28. Li, H. S. et al. HIF-1α protects against oxidative stress by directly targeting mitochondria. *Redox Biol.* **25**, 101109. https://doi.org/10.1016/j.redox.2019.101109 (2019).
29. Jing, L. et al. Protective effects of two novel nitronyl nitroxide radicals on heart failure induced by hypobaric hypoxia. *Life Sci.* **248**, 116481. https://doi.org/10.1016/j.lfs.2019.05.037 (2020).
30. Niecknig, H. et al. Role of reactive oxygen species in the regulation of HIF-1 by prolyl hydroxylase 2 under mild hypoxia. *Free Radic Res.* **46**, 705–717. https://doi.org/10.3109/10715762.2012.669041 (2012).
31. Chen, R. et al. Necrostatin-1 protects C2C12 myotubes from CoCl2-induced hypoxia. *Int. J. Mol. Med.* **41**, 2565–2572. https://doi.org/10.3892/ijmm.2018.3466 (2018).
32. Yan, C. et al. Resveratrol ameliorates high Altitude Hypoxia-Induced osteoporosis by suppressing the ROS/HIF signaling pathway. *Molecules* **27**, 5538. https://doi.org/10.3390/molecules27175538 (2022).
33. Malkov, M. I., Lee, C. T. & Taylor, C. T. Regulation of the Hypoxia-Inducible factor (HIF) by pro-inflammatory cytokines. *Cells* **10** https://doi.org/10.3390/cells10092340 (2021).
34. Lawrence, T. The nuclear factor NF-kappaB pathway in inflammation. *Cold Spring Harb Perspect. Biol.* **1**, a001651. https://doi.org/10.1101/cshperspect.a001651 (2009).
35. Van Quickelberghe, E., De Sutter, D., van Loo, G. & Eyckerman, S. Gevaert K. A protein-protein interaction map of the TNF-induced NF-κB signal transduction pathway. *Sci. Data.* **5**, 180289. https://doi.org/10.1038/sdata.2018.289 (2018).
36. Wang, X., Li, J., Wu, D., Bu, X. & Qiao, Y. Hypoxia promotes apoptosis of neuronal cells through hypoxia-inducible factor-1α-microRNA-204-B-cell lymphoma-2 pathway. *Exp. Biol. Med. (Maywood).* **241**, 177–183. https://doi.org/10.1177/1535370215600548 (2016).
37. Lossi, L. The concept of intrinsic versus extrinsic apoptosis. *Biochem. J.* **479**, 357–384. https://doi.org/10.1042/bcj20210854 (2022).
38. Kesavardhana, S., Malireddi, R. K. S. & Kanneganti, T. D. Caspases in cell death, inflammation, and Pyroptosis. *Annu. Rev. Immunol.* **38**, 567–595. https://doi.org/10.1146/annurev-immunol-073119-095439 (2020).
39. Zhang, Q. et al. Activation of Nrf2/HO-1 signaling: an important molecular mechanism of herbal medicine in the treatment of atherosclerosis via the protection of vascular endothelial cells from oxidative stress. *J. Adv. Res.* **34**, 43–63. https://doi.org/10.1016/j.jare.2021.06.023 (2021).
40. Guo, H. et al. Identifying key antioxidative stress factors regulating Nrf2 in the genioglossus with human umbilical cord mesenchymal stem-cell therapy. *Sci. Rep.* **14**, 5838. https://doi.org/10.1038/s41598-024-55103-8 (2024).
41. Han, X. et al. 6-Gingerol exerts a protective effect against hypoxic injury through the p38/Nrf2/HO-1 and p38/NF-κB pathway in H9c2 cells. *J. Nutr. Biochem.* **104**, 108975. https://doi.org/10.1016/j.jnutbio.2022.108975 (2022).
42. Wang, Y., Zhang, L. & Zhou, X. Activation of Nrf2 signaling protects hypoxia-induced HTR-8/SVneo cells against ferroptosis. *J. Obstet. Gynaecol. Res.* **47**, 3797–3806. https://doi.org/10.1111/jog.15009 (2021).
43. Kolamunne, R. T., Dias, I. H., Vernallis, A. B., Grant, M. M. & Griffiths, H. R. Nrf2 activation supports cell survival during hypoxia and hypoxia/reoxygenation in cardiomyoblasts; the roles of reactive oxygen and nitrogen species. *Redox Biol.* **1**, 418–426. https://doi.org/10.1016/j.redox.2013.08.002 (2013).
44. Zafar, S. et al. Daidzein attenuated paclitaxel-induced neuropathic pain via the down-regulation of TRPV1/P2Y and up-regulation of Nrf2/HO-1 signaling. *Inflammopharmacology* **31**, 1977–1992. https://doi.org/10.1007/s10787-023-01225-w (2023).
45. Shirvanian, K. et al. Genistein effects on various human disorders mediated via Nrf2 Signaling. *Curr. Mol. Med.* **24**, 40–50. https://doi.org/10.2174/1566524023666221128162753 (2024).
46. Lu, C. Y. et al. Calycosin alleviates H(2) O(2) -induced astrocyte injury by restricting oxidative stress through the Akt/Nrf2/HO-1 signaling pathway. *Environ. Toxicol.* **37**, 858–867. https://doi.org/10.1002/tox.23449 (2022).
47. Liang, F. et al. Isoflavone biochanin A, a novel nuclear factor erythroid 2-related factor 2 (Nrf2)-antioxidant response element activator, protects against oxidative damage in HepG2 cells. *Biofactors* **45**, 563–574. https://doi.org/10.1002/biof.1514 (2019).

Author contributions

All authors contributed to conceptualization. Investigation and methodology were carried out by P.Z., and J.Z. Material preparation and formal analysis were performed by P.Z., C.M., and L.J. Project administration and resources were conducted by H.M., and L.J. The original draft was written by P.Z., J.Z., C.M., and L.J. The manuscript was revised by H.M., and L.J. All authors read and approved the final manuscript.

Funding

The present study is funded by the Military Logistics Research Project (2023HQZZ-02), Special Cultivation Project of the 940th Hospital of Joint Logistics Support force of PLA (2021yxky015) and Institutional Foundation of The First Affiliated Hospital of Xi'an Jiaotong University (2022MS-11).

Declarations

Competing interests
The authors declare no competing interests.

Additional information
Supplementary Information The online version contains supplementary material available at https://doi.org/10.1038/s41598-025-85286-7.

Correspondence and requests for materials should be addressed to H.M. or L.J.

Reprints and permissions information is available at www.nature.com/reprints.

Publisher's note Springer Nature remains neutral with regard to jurisdictional claims in published maps and institutional affiliations.